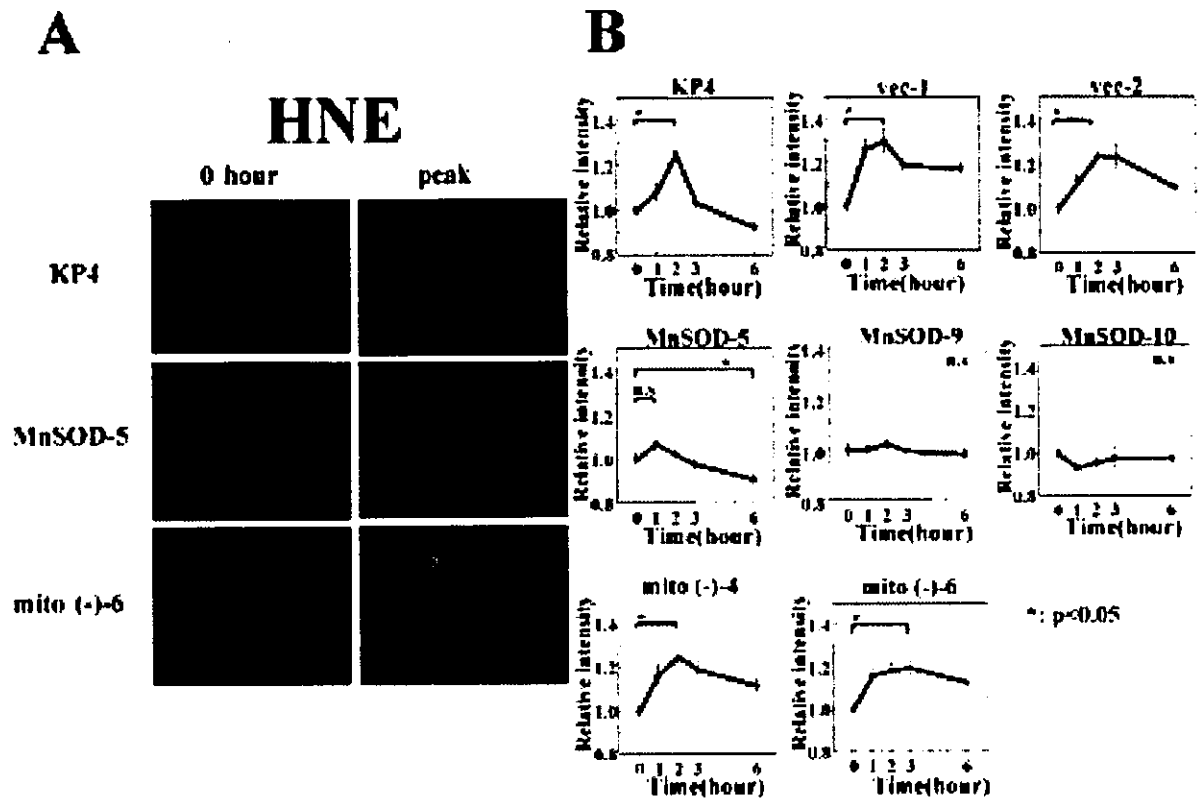

FIG. 7. Intracellular HNE adducts. The intracellular levels of HNE protein adducts in each cell line at 0, 1, 2, 3, and 6 h in air after 1 day of hypoxia treatment (H/R treatment) were determined. **(A)** Representative photographs of cell staining with an antibody against HNE protein adducts at 0 h or peak hours. **(B)** Relative fluorescent intensity of HNE protein adducts versus time (hours) in air following 1 day of hypoxia treatment (H/R treatment). n.s, not significant; $*p < 0.05$.

DISCUSSION

Using a human pancreatic tumor cell line, KP4, we first examined the effects of H/R on ROS production, lipid peroxidation, and cellular viability following 1 day of hypoxia and subsequent exposure to air. The results show that H/R increased ROS, lipid peroxidation, and apoptosis, although the apoptosis frequency was small. In this study, we investigated whether an enhanced expression of mitochondrial MnSOD, a superoxide-scavenging enzyme, can protect cells against H/R.

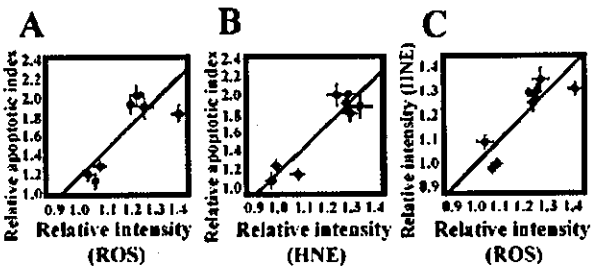

FIG. 8. Correlation between mitochondrial ROS, intracellular lipid peroxidation protein adducts, and cell death. (A) Linear-regression analysis showing the relationship between the relative apoptosis index and the relative dhRho staining intensity (mitochondrial ROS) after H/R treatment ($r = 0.818$, $p = 0.018$). **(B)** Relationship between the relative apoptosis index and the relative HNE protein-adducts staining intensity (intracellular lipid peroxidation products) ($r = 0.933$, $p = 0.018$). **(C)** Relationship between the relative dhRho staining intensity and the relative HNE protein adducts staining ($r = -0.856$, $p = 0.020$). Mitochondrial ROS, intracellular lipid peroxidation products, and apoptosis have a strong correlation with each other.

We found that H/R-produced apoptosis is suppressed by MnSOD, but not by mito(−) MnSOD, which is not located in the mitochondria. These results signify the importance of mitochondrial localization of MnSOD. It has been shown that adenoviral gene transfer with MnSOD is effective in reducing the extent of *in vivo* I/R injury in the rat heart (1) and in mouse liver (50), but expression of copper/zinc SOD (Cu/ZnSOD) did not function in protection in the mouse liver model (50). Given the fact that the MnSOD and Cu/ZnSOD used in these studies were mainly expressed in the mitochondria and cytosol, respectively, these results are consistent with our results. Our results further indicate that not only is active MnSOD important, but also it must be located in the mitochondria for the observed protection.

The reaction between superoxide radicals and NO to form peroxynitrite is a subject under considerable study. Superoxide radicals can react at diffusion rates with NO to form peroxynitrite, a potent biological oxidant. In this study, however, we could not find evidence of further NO induction by hypoxia treatment. This is not surprising, because oxygen is an essential substrate for NO synthesis. Our results are also consistent with various other reports that indicate that hypoxia

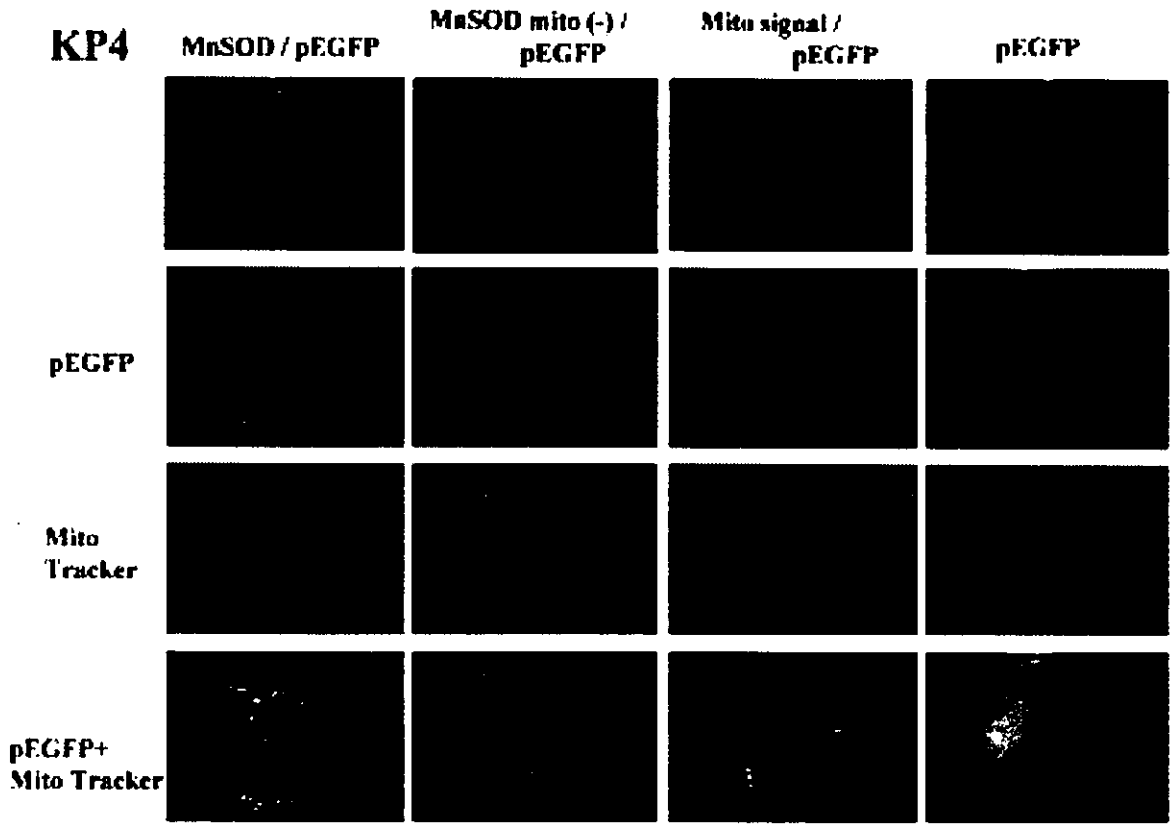

FIG. 9. Localization of MnSOD, MnSOD lacking MTS, and MTS alone in KP4 cells. Localization of full-length MnSOD, MnSOD lacking MTS [MnSOD mito (−)], and MTS signal alone (Mito signal) is shown. GFP was visualized using the pEGFP transfection sytem. To locate mitochondria, the same cells were stained with MitoTracker Red CMXRos. Merged double images of GFP and MitoTracker were made to identify MnSOD in mitochondria. MnSOD was localized in mitochondria, as shown by the yellow color (green plus red) in the double image of pEGFP and MitoTracker. A similar image was taken for MTS alone (Mito signal) in the double image, where a yellow color is clearly shown. However, for MTS lacking MnSOD [MnSOD mito (−)], only a few yellow color regions can be seen in the double color picture, indicating that most of the MnSOD lacking MTS was localized in cytosol, although the fluorescent intensity of pEGFP is unclear or obscure in cytosol in the picture.

limits NO synthesis even when NO synthase is overexpressed (for review, see 19). As ROS are increased without a concurrent increase in NO production in the H/R model, it is likely that the observed increase in HNE-modified proteins is mediated via hydroxyl radical generation. The finding that increased expression of MnSOD abolished the increased levels of HNE-modified proteins under H/R further supports this possibility.

Our results indicating that only MnSOD and not mito(−) transfectants suppress the formation of HNE-modified proteins suggest that superoxide production in the mitochondria is important for the production of HNE-modified proteins under conditions of H/R. Our results further indicate that the localization of active MnSOD in the mitochondrion is important for the suppression of ROS production and subsequent formation of HNE protein adducts. These results suggest that H/R-induced apoptosis is linked to the production of ROS and its toxic products.

Mitochondrial damage and the role of mitochondria in apoptosis are well established in various pathological conditions. However, it is largely unknown whether mitochondria are the sources or targets in such apoptosis events. Our results suggest that induction of oxidative injury in mitochondria is an upstream event leading to apoptosis in H/R-induced cell death.

Endogenous MnSOD is a nuclear-encoded protein that is cotranslationally transported into mitochondria where the signal peptide is removed and Mn is inserted to produce active proteins. The role of MnSOD in protecting against oxidative stress-mediated cell death has been demonstrated in organisms ranging from bacteria to mammals. In all studies reported thus far, it has been assumed that the effect of MnSOD is due to its location in mitochondria. However, the question remains to be investigated as to whether enzyme localized outside mitochondria has any protective effect. Our results reported here clearly demonstrate that expression of active MnSOD outside mitochondria was not effective. Although it is unclear how MnSOD located outside mitochondria acquires its Mn and proper conformation for its activity, our results from activity assay, mRNA RT-PCR assay, apoptosis observation, and colocalization studies (Table 1, Figs. 2, 4, and 9) provide strong support that active MnSOD outside mitochondria is not effective in protecting against H/R-induced apoptosis. Our GFP vector images (Fig. 9) show that

only small amounts of transfectants of MnSOD mito(−) are found in mitochondria. The distribution of GFP outside mitochondria of the MnSOD and Mito signal alone may indicate that the intensity of MnSOD lacking MTS was low because of a wide dispersion over cytosol. Although our finding that the MnSOD construct lacking MTS expresses active MnSOD protein outside mitochondria is unexpected; this phenomenon has been observed for other antioxidant enzymes as well. For example, Tamura *et al.*(37) demonstrated a much greater enhancement of cellular resistance to oxidant challenge by CHO cells by stable transfection with leader sequence of glutathione reductase (GR) cDNA than they observed in a construct lacking the MTS, which produced comparable increases in the total cellular GR activities, but did not increase mitochondrial GR activities (29, 37, 38). Arai *et al.* (2) demonstrated the effect of phospholipid hydroperoxide glutathione peroxidase, which is naturally synthesized as a long form (the L-form; 23 kDa) and a short form (the S-form; 20 kDa). The long form contains a mitochondrial targeting leader sequence, whereas the short form lacks the leader sequence. Cells transfected with the L-form containing vector were more resistant against oxidative stress, including potassium cyanide, rotenone (chemical hypoxia), and exogenous *tert*-butyl hydroperoxide oxidant injuries, compared with those cells transfected with the S-form containing vector (2). Wong (46) demonstrated that MnSOD without the mitochondrial leading targeting signal failed to protect against radiation, whereas the reduction of normal cytosolic Cu/ZnSOD or normally extracellularly expressed SOD to mitochondria with MTS resulted in protection against radiation. These results suggest that MnSOD, which is located in cytosol, does not function to prevent against H/R treatment-induced oxidative damage and cell death, and only when the enzyme is located in mitochondria does MnSOD have a function. Taken together, these data support the critical role of mitochondria localization of antioxidant enzymes for the protection against cellular injury from outside stress initiated in the mitochondrion.

In summary, the findings shown in study indicated that (a) H/R induced increased mitochondrial ROS production, lipid peroxidation protein-adducts, and subsequent apoptosis; (b) these processes were suppressed by active MnSOD in the mitochondria but not in the cytosol even when the MnSOD is active; and (c) the results support the overall hypothesis depicted in Fig. 10 showing that H/R triggers mitochondrial ROS production and generation of lipid peroxidation products, and subsequently accelerates cell death and its inhibition by MnSOD.

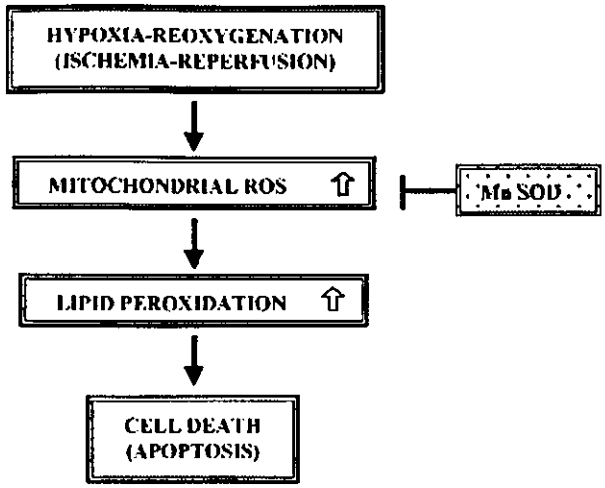

FIG. 10. Schematic diagram of a hypothesis on how ROS generation and lipid peroxidation products affect cell death (apoptosis) and its prevention by MnSOD after H/R treatment.

ACKNOWLEDGMENTS

The authors wish to thank Dr. Makoto Akashi (NIRS) for MnSOD cDNA, and Ms Chizuru Yamaguchi and Dr. Yoichiro Iwashita for technical assistance. This study was partially supported by "Ground Research Announcement for Space Utilization" promoted by Japan Space Forum, and The Nuclear Cross-Over Research Study, Grant-in Aid for Scientific Research (C) (2) #10671786, #12671844, #14207078, and #15659451 of Ministry of Education, Culture, Sports, Science and Technology, Japan.

ABBREVIATIONS

Cu/ZnSOD, copper/zinc superoxide dismutase; DAF, diaminofluorescein; DAF-FM DA, diaminofluorescein-FM diacetate; dhRho, dihydrorhodamine 123; DMEM, Dulbecco's modified Eagle medium; GFP, green fluorescent protein; GR, glutathione reductase; HNE, 4-hydroxy-2-nonenal; H/R, hypoxia followed by reoxygenation; I/R, ischemia/reperfusion; mito(−), lacking MTS; mito(−)-, MTS lacking MnSOD transfected cell clone; MnSOD, manganese superoxide dismutase (EC 1.15.1.1); MnSOD-, MnSOD transfected cell clone; MTS, mitochondrial targeting signal; NO, nitric oxide; PBS, phosphate-buffered saline; ROS, reactive oxygen species; SOD, superoxide dismutase; vec-, vector alone transfected cell clone.

REFERENCES

1. Abunasra HJ, Smolenski RT, Morrison K, Yap J, Sheppard MN, O'Brien T, Suzuki K, Jayakumar J, and Yacoub MH. Efficacy of adenoviral gene transfer with manganese superoxide dismutase and endothelial nitric oxide synthase in reducing ischemia and reperfusion injury. *Eur J Cardiothorac Surg* 20: 153–158, 2001.
2. Arai M, Imai H, Koumura T, Yoshida M, Emoto K, Umeda M, Chiba N and Nakagawa Y. Mitochondrial phospholipid hydroperoxide glutathione peroxidase plays a major role in preventing oxidative injury to cells. *J Biol Chem* 274: 4924–4933, 1999.
3. Beauchamp C and Fridovich I. Superoxide dismutase: improved assays and an assay applicable to acrylamide gels. *Anal Biochem* 44: 276–287, 1971.
4. Bienvenu P, Caron L, Gasparutto D, and Kergonou JF. Assessing and counteracting the prooxidant effects of anticancer drugs. *EXS* 62: 257–265, 1992.

5. Boveris A and Cadenas E. Mitochondrial production of superoxide anions and its relationship to the antimycin insensitive respiration. *FEBS Lett* 1: 311–314, 1975.
6. Brown JM. Evidence for acutely hypoxic cells in mouse tumours, and a possible mechanism of reoxygenation. *Br J Radiol* 52: 650–656, 1979.
7. Brown JM. The hypoxic cell: a target for selective cancer therapy—eighteenth Bruce F. Cain Memorial Award lecture. *Cancer Res* 59: 5863–5870, 1999.
8. Carlioz A and Touati D. Isolation of superoxide dismutase mutants in *Escherichia coli:* is superoxide dismutase necessary for aerobic life? *EMBO J* 5: 623–630, 1986.
9. Chomczynski P and Sacchi N. Single-step method of RNA isolation by acid guanidinium thiocyanate–phenol–chloroform extraction. *Anal Biochem* 162: 156–159, 1987.
10. Engelhardt JF. Redox-mediated gene therapies for environmental injury: approaches and concepts. *Antioxid Redox Signal* 1: 5–27, 1999.
11. Farr SB, D'Ari R, and Touati D. Oxygen-dependent mutagenesis in *Escherichia coli* lacking superoxide dismutase. *Proc Natl Acad Sci USA* 83: 8268–8272, 1986.
12. Halliwell B and Gutteridge JMC. Free radicals, other reactive species and disease. In: *Free Radicals in Biology and Medicine.* 3rd edit., edited by Halliwell B and Gutteridge JMC. Oxford, U.K.: Oxford University Press, 1999, pp.617–783.
13. Hirose K, Longo DL, Oppenheim JJ, and Matsushima K. Overexpression of mitochondrial manganese superoxide dismutase promotes the survival of tumor cells exposed to interleukin-1, tumor necrosis factor, selected anticancer drugs, and ionizing radiation. *FASEB J* 7: 361–368, 1993.
14. Ho YS and Crapo JD Isolation and characterization of complementary DNAs encoding human manganese-containing superoxide dismutase. *FEBS Lett* 229: 256–260, 1988.
15. Kiningham KK, Oberley TD, Lin S, Mattingly CA, and St Clair DK. Overexpression of manganese superoxide dismutase protects against mitochondrial-initiated poly(ADP-ribose) polymerase-mediated cell death. *FASEB J* 13: 1601–1610, 1999.
16. Knisely JP and Rockwell S. Importance of hypoxia in the biology and treatment of brain tumors. *Neuroimaging Clin N Am* 12: 526–536, 2002.
17. Kojima H, Nakatsubo N, Kikuchi K, Kawahara S, Kirino Y, Nagoshi H, Hirata Y, and Nagano T. Detection and imaging of nitric oxide with novel fluorescent indicators: diaminofluoresceins. *Anal Chem* 70: 2446–2453, 1998.
18. Lebovitz RM, Zhang H, Vogel H, Cartwright J Jr, Dionne L, Lu N, Huang S, and Matzuk MM. Neurodegeneration, myocardial injury, and perinatal death in mitochondrial superoxide dismutase deficient mice. *Proc Natl Acad Sci U S A* 93: 9782–9787, 1996.
19. Le Cras TD and McMurtry IF. Nitric oxide production in the hypoxic lung. *Am J Physiol Lung Cell Mol Physiol* 280: L575–L582, 2001.
20. Lee JM, Zipfel GJ, and Choi DW. The changing landscape of ischaemic brain injury mechanisms. *Nature* 399 (6738 Suppl): A7–A14, 1999.
21. Li Y, Huang T-T, Carlson EJ, Melov S, Ursell PC, Olson JL, Noble LJ, Yoshimura MP, Berger C, Chan PH, Wallace DC, and Epstein CJ. Dilated cardiomyopathy and neonatal lethality in mutant mice lacking manganese superoxide dismutase. *Nat Genet* 11: 376–381, 1995.
22. Lithgow T. Targeting of proteins to mitochondria. *FEBS Lett* 476: 22–26, 2000.
23. Majima HJ, Oberley TD, Furukawa K, Mattson MP, Yen HC, Szweda LI, and St. Clair DK. Prevention of mitochondrial injury by manganese superoxide dismutase reveals a primary mechanism for alkaline-induced cell death. *J Biol Chem* 273: 8217–8224, 1998.
24. Mattson MP. Apoptosis in neurodegenerative disorders. *Nat Rev Mol Cell Biol* 1: 120–129, 2000.
25. Mattson MP, Duan W, Pedersen WA, and Culmsee C. Neurodegenerative disorders and ischemic brain diseases. *Apoptosis* 6: 69–81, 2001.
26. Mihara T and Onuma T. Cytoplasmic chaperons in precursor targeting to mitochondria: the role of MSF and hsp70. *Trends Cell Biol* 6: 104–108, 1996.
27. Motoori S, Majima HJ, Ebara M, Kato H, Hirai F, Kakinuma S, Yamaguchi C, Ozawa T, Nagano T, Tsujii H, and Saisho H. Overexpression of mitochondrial manganese superoxide dismutase protects against radiation-induced cell death in the human hepatocellular carcinoma cell line HLE. *Cancer Res* 61: 5382–5388, 2001.
28. Nishi Y, Haji M, Takayanagi R, Iguchi H, Shimazoe T, Hirata J, and Nawata H. Establishment of characterization of PTHrP-producing human pancreatic cancer cell line. *Int J Oncol* 5: 33–39, 1994.
29. O'Donovan DJ, Katkin JP, Tamura T, Husser R, Xu X, Smith CV, and Welty SE. Gene transfer of mitochondrially targeted glutathione reductase protects H441 cells from *t*-butyl hydroperoxide-induced oxidant stresses. *Am J Respir Cell Mol Biol* 20: 256–263, 1999.
30. Riley PA. Free radicals in biology: oxidative stress and the effects of ionizing radiation. *Int J Radiat Biol* 65: 27–33, 1994.
31. Rofstad EK. Microenvironment-induced cancer metastasis. *Int J Radiat Biol* 76: 589–605, 2000.
32. St Clair DK, Oberley TD, and Ho Y-S. Overproduction of human Mn-superoxide dismutase modulates paraquat-mediated toxicity in mammalian cells. *FEBS Lett* 293: 199–203, 1991.
33. St. Clair DK, Wan XS, Oberley TD, Muse KE, and St Clair WH. Suppression of radiation-induced neoplastic transformation by overexpression of mitochondrial superoxide dismutase. *Mol Carcinog* 6: 238–242, 1992.
34. St Clair DK, Jordan JA, Wan S, and Gairola CG. Protective role of manganese superoxide dismutase against cigarette smoke-induced cytotoxicity. *J Toxicol Environ Health* 43: 239–249, 1994.
35. Sun J, Chen Y, Li M, and Ge Z. Role of antioxidant enzymes on ionizing radiation resistance. *Free Radic Biol Med* 24: 586–593, 1998.
36. Takeshige K and Minakami S. NADH- and NADPH-dependent formation of superoxide anions by bovine heart submitochondrial particles and NADH-ubiquinone reductase preparation. *Biochem J* 180: 129–135, 1979.
37. Tamura T, McMicken HW, Smith CV, and Hansen TN. Mitochondrial targeting of glutathione reductase requires a leader sequence. *Biochem Biophys Res Commun* 222: 659–663, 1996.

38. Tamura T, McMicken HW, Smith CV, and Hansen TN. Gene structure for mouse glutathione reductase, including a putative mitochondrial targeting signal. *Biochem Biophys Res Commun* 237: 419–422, 1997.
39. Thomlinson RH and Gray LH. The histological structure of some human lung cancers and the possible implications for radiotherapy. *Br J Cancer* 9: 539–549, 1955.
40. Toyokuni S, Miyake N, Hiai H, Hagiwara M, Kawakishi S, Osawa T, and Uchida K. The monoclonal antibody specific for the 4-hydroxy-2-nonenal histidine adduct. *FEBS Lett* 359: 189–191, 1995.
41. van Loon APGM, Pesold-Hurt B, and Schatz G. A yeast mutant lacking mitochondrial manganese-superoxide dismutase is hypersensitive to oxygen. *Proc Natl Acad Sci US A* 83: 3820–3824, 1986.
42. van Putten LM. Tumor reoxygenation during fractionated radiotherapy: studies with a transplantable osteosarcoma. *Eur J Cancer* 4: 173–182, 1968.
43. Wallace DC. Mitochondrial DNA in aging and disease. *Sci Am* 277: 40–47, 1997.
44. Weisiger RA and Fridovich I. Mitochondrial superoxide disimutase. Site of synthesis and intramitochondrial localization. *J Biol Chem* 248: 4793–4796, 1973.
45. Wispe JR, Warner BB, Clark JC, Dey CR, Neuman J, Glasser SW, Crapo JD, Chang L-Y, and Whitsett JA. Human Mn-superoxide dismutase in pulmonary epithelial cells of transgenic mice confers protection from oxygen injury. *J Biol Chem* 267: 23937–23941, 1992.
46. Wong GH. Protective roles of cytokines against radiation: induction of mitochondrial MnSOD. *Biochim Biophys Acta* 1271: 205–209, 1995.
47. Wong GHW, Elwell JH, Oberley LW, and Goeddel DV. Manganous superoxide dismutase is essential for cellular resistance to cytotoxicity of tumor necrosis factor. *Cell* 58: 923–931, 1989.
48. Yen H-C, Oberley TD, Vichitbandha S, Ho Y-S, and St Clair DK. The protective role of manganese superoxide dismutase against adriamycin-induced acute cardiac toxicity in transgenic mice. *J Clin Invest* 98: 1253–1260, 1996.
49. Yen H-C, Nien C-Y, Majima HJ, Lee C-P, Chen S-Y, Wei J-S, and See L-C. Increase of lipid peroxidation by cisplatin in WI38 cells but in SV40-transformed WI38 cells. *J Biochem Mol Toxicol* 17: 39–46, 2003.
50. Zhou W, Zhang Y, Hosch MS, Lang A, Zwacka RM, and Engelhardt JF. Subcellular site of superoxide dismutase expression differentially controls AP-1 activity and injury in mouse liver following ischemia/reperfusion. *Hepatology* 33: 902–914, 2001.

Address reprint requests to:
Hideyuki J. Majima, D.D.S., Ph.D.
Department of Oncology and Department of Space Environmental Medicine
Kagoshima University Graduate School of Medical and Dental Sciences
Kagoshima 890-8544, Japan

E-mail: hmajima@denta.hal.kagoshima-u.ac.jp

Received for publication October 18, 2003; accepted February 19, 2004.

Evaluation of anti-platelet aggregatory effects of aspirin, cilostazol and ramatroban on platelet-rich plasma and whole blood

Hiroko Kariyazono[a], Kazuo Nakamura[a], Junko Arima[a], Osamu Ayukawa[a], Shunji Onimaru[a], Hiroshi Masuda[b], Yoshifumi Iguro[b], Hideyuki J. Majima[c], Ryuzo Sakata[b] and Katsushi Yamada[a]

To compare property in anti-platelet effects of aspirin (a cyclooxygenase inhibitor), cilostazol (a phosphodiesterase III inhibitor) and ramatroban (a specific thromboxane A_2 receptor antagonist), we measured human platelet-rich plasma (PRP) aggregation induced by adenosine diphosphate (ADP), collagen and arachidonic acid, and whole blood (WB) aggregation induced by ADP. The release of P-selectin, transforming growth factor-beta 1, and the formation of thromboxane A_2 in response to agonists were also investigated. Inhibitory effects of 100 μmol/l aspirin, 10 μmol/l cilostazol and 1 μmol/l ramatroban on 5 μmol/l ADP-induced PRP aggregation were similar. However, aspirin strongly inhibited thromboxane A_2 formation in response to 5 μmol/l ADP compared with other drugs. Inhibitory effects of 10 μmol/l cilostazol on PRP aggregation and the release of molecules were quite similar in responsiveness induced by the three agonists. Aspirin and cilostazol inhibited platelet aggregation in a concentration-dependent, non-linear fashion, while ramatroban inhibited linearly with increasing concentration. Anti-platelet effects of drugs having different pharmacological mechanisms were demonstrated clearly by measuring PRP aggregation induced by the three agonists, and by measuring WB aggregation that most probably reflects not only platelet–platelet interactions, but also platelet–leukocyte interactions, as well as the release of intraplatelet molecules. *Blood Coagul Fibrinolysis* **15:157–167 © 2004 Lippincott Williams & Wilkins.**

Blood Coagulation and Fibrinolysis 2004, 15:157–167

Keywords: whole blood aggregation, platelet-rich plasma, aspirin, cilostazol, ramatroban

[a]Department of Clinical Pharmacy and Pharmacology, [b]Department of Thoracic Cardiovascular Surgery, Hepato-Biliary-Pancreatic Surgery, and [c]Department of Oncology, Division of Maxillofacial Radiology and Department of Space Environmental Medicine, Graduate School of Medical and Dental Sciences, Kagoshima University, Kagoshima, Japan.

Sponsorship: This study was supported in part by grant-in-aid for scientific research 13672395 from the Ministry of Education, Culture, Sports, Science and Technology, Japan.

Correspondence and requests for reprints to Kazuo Nakamura, Department of Clinical Pharmacy and Pharmacology, Graduate School of Medical and Dental Sciences, Kagoshima University 8-35-1 Sakuragaoka, Kagoshima 890-8520, Japan.
Tel: +81 99 275 5542; fax: +81 99 265 5293;
e-mail: knaka@denta.hal.kagoshima-u.ac.jp

Received 28 January 2003 Revised 26 August 2003
Accepted 4 November 2003

Introduction

Anti-platelet drugs are administered to prevent the formation of thrombus due to platelet activation in patients with myocardial infarction, thrombotic strokes and peripheral vascular disease [1,2]. It is necessary to manage the effects of anti-platelet drugs to within an appropriate therapeutic range to protect patients from the formation of thrombus and bleeding. Measurement of platelet aggregation has been widely carried out to assess platelet function and the effects of anti-platelet drugs. By far the most common method to detect platelet aggregation is by measuring light transmission of platelet-rich plasma (PRP) [3], while another method to detect platelet aggregates in PRP is a light-scattering method based on a particle counting [4,5]. There are also some methods using whole blood (WB) such as electrical impedance aggregometry [6,7], measurement of closure time of an artificial vessel with a bioactive membrane having a microscopic aperture [3,8], light absorbance measurement of blood samples based on agglutination of platelets to fibrinogen-coated beads [3,9,10], and a screen filtration pressure method that measures platelet aggregation in terms of increasing resistance of WB sample flow through a microsieve [11,12]. Notably, the screen filtration pressure method has not been widely utilized to date, largely due to the difficulty of measurement of screen filtration pressure, causing problems with reproducibility and difficulty in the measurement of platelet aggregation. Platelet aggregation is probably mediated by platelet–leukocyte interactions regulated by chemical mediators from leukocytes, erythrocytes and other cells [13,14]. Therefore, it is believed that platelet aggregation in WB could possibly reflect physiological conditions more accurately than aggregation in PRP. Recently, a new type of WB aggregometer with a screen filtration

0957-5235 © 2004 Lippincott Williams & Wilkins

DOI: 10.1097/01.mbc.0000114383.15192.ee

diameter area. The final platelet aggregation pressure of each reaction tube was determined as the pressure rate of a pressure sensor connected to the syringe. The pressure rate was standardized by a grading curve; 1, 2, 4 and 8 μmol/l ADP were plotted on the *x* axis and the pressure rates (%) were plotted on the *y* axis. Figure 1 shows a representative analysis of platelet aggregation by the WB aggregometer using a grading curve. The concentration of ADP inducing a 50% pressure rate was calculated and indicated as the platelet aggregatory threshold index (PATI). PATI values were used to evaluate WB aggregation.

Time course change in the PATI after blood collection and reproducibility in WB aggregation

To investigate changes in the PATI after blood collection over time, WB aggregation was measured at 5, 15, 30, 60 and 120 min after blood collection in eight healthy volunteers. The reproducibility of WB aggregation was also examined in blood samples. At 60 min after blood collection, the PATI values determined from WB on one day were compared with values from another day when the same measurements were performed.

Fig. 1

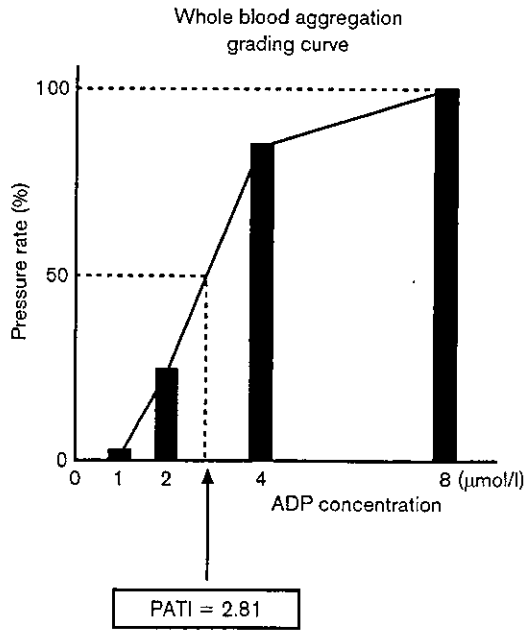

A representative analysis of whole blood aggregation using a grading curve. The *x* axis is adenosine diphosphate (ADP) concentration, and the *y* axis is pressure rate (%). The concentration of ADP inducing 50% pressure rate was calculated and indicated as a platelet aggregatory threshold index value. Whole blood aggregation was measured at 60 min after blood collection. PATI, platelet aggregatory threshold index.

Estimation of drug effects on WB aggregation and its comparison with PRP aggregation

At 60 min after blood collection, the working solutions of aspirin, cilostazol and ramatroban were added to WB, followed by incubation for 3 min. Drug-treated WB was stimulated by ADP and WB aggregation was measured as already described. In addition, PATI values in PRP aggregation were also calculated from light transmission 5 min after ADP addition in a similar manner to WB (Fig. 2), and were compared with those in WB aggregation.

Co-existence of platelets and leukocytes on the microsieve

To investigate the co-existence of platelets and leukocytes on the microsieve after WB aggregometry, staining of platelets and leukocytes was performed by use of dual-colour immunofluorescence. Erythrocytes on the microsieve were lysed with lysis buffer containing NH_4Cl, $NaHCO_3$ and EDTA2Na, and then were fixed with commercially available solution (Cell Fix; Becton Dickinson, San Jose, California, USA). After being washed three times, the microsieves were pre-incubated with 5% bovine serum albumin in phosphate-buffered saline (pH 7.4) at room temperature. After removing the solution, the microsieves were incubated with saturating concentrations of PE-conjugated anti-CD42b and FITC-conjugated anti-CD45 in a total volume of 500 μl phosphate-buffered saline containing 2% bovine serum albumin for 4 h at 4°C in the dark, then washed five times with phosphate-buffered saline. Images of the immunofluorescent samples were obtained using a CSU-10 confocal laser scanning unit (Yokogawa Electric Co., Tokyo, Japan) coupled to an IX90 inverted microscope with UPlanAPO × 20 objective lens (Olympus Optical Co., Tokyo, Japan) and a C5810-01 colour chilled 3CCD camera (Hamamatsu Photonics K. K., Hamamatsu, Japan) [30,31].

Statistical analysis

The data are expressed as means ± standard deviation. Statistical analysis was performed by a one-way analysis of variance, which was followed by Fisher's protected least significant difference test. Relationships between independent variables were assessed by Pearson's correlation. Differences were considered to be significant at $P < 0.05$. StatView J-4.5 software (Abacus Concepts Inc., Berkeley, California, USA) was employed for all calculations.

Results

Inhibitory effects of aspirin, cilostazol and ramatroban on PRP aggregation

MA values from control PRP in response to ADP (1 and 5 μmol/l), collagen (1 μg/ml) and arachidonic acid (3 mmol/l) are presented in Table 1. When control PRP was stimulated by 1 μmol/l ADP, primary aggregation was induced in all specimens, with MAs of 40% or less,

Fig. 3

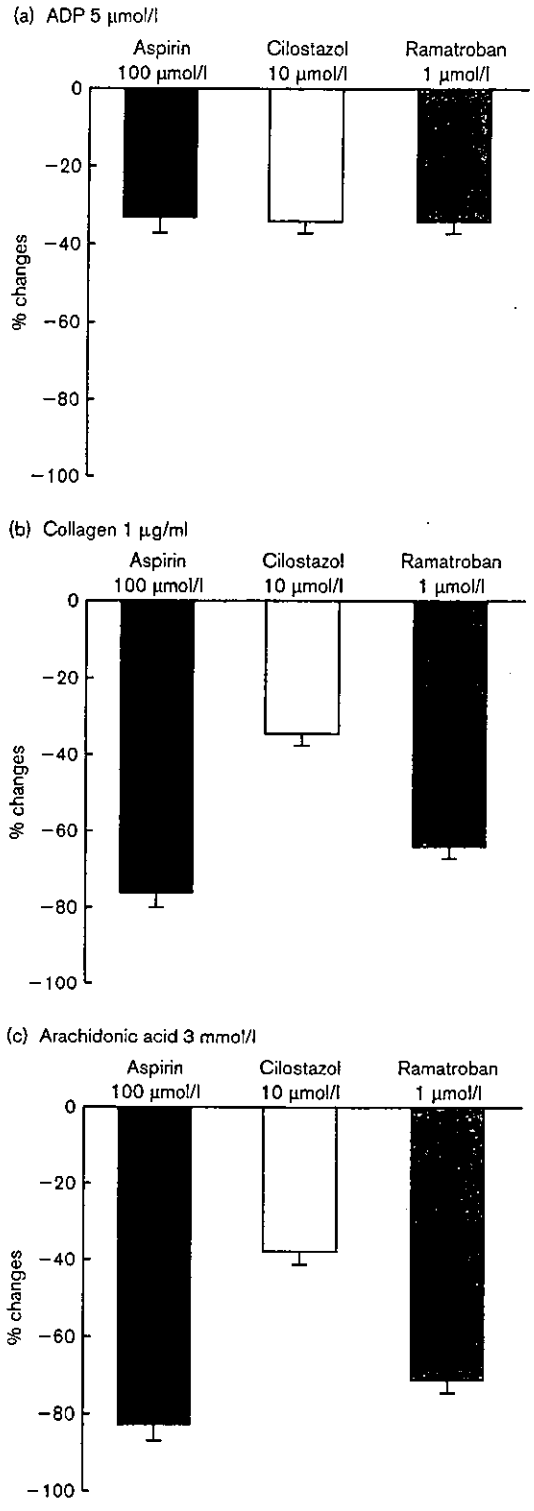

Inhibitory effects of aspirin, cilostazol and ramatroban on platelet-rich plasma (PRP) aggregation induced by (a) adenosine diphosphate (ADP) (5 μmol/l), (b) collagen (1 μg/ml) and (c) arachidonic acid (3 mmol/l). PRP samples were pre-incubated with drugs for 3 min prior to the addition of agonists. Effects of drugs were evaluated as percentage changes in maximum aggregation against vehicle-treated samples. Data represent mean ± standard deviation ($n = 8$).

was stimulated by 1 μmol/l ADP, sP-selectin and TGF-β1 levels increased significantly compared with their circulating plasma levels ($P < 0.05$). TXB_2 also showed high levels, although no difference was found between the levels in response to 1 μmol/l ADP and the levels in circulating plasma. The levels of sP-selectin, TGF-β1 and TXB_2 in response to 5 μmol/l ADP, collagen (1 μg/ml) and arachidonic acid (3 mmol/l) were significantly higher than those in response to 1 μmol/l ADP ($P < 0.001$). Furthermore, TXB_2 levels in response to arachidonic acid markedly increased compared with those in response to 5 μmol/l ADP ($P < 0.001$).

The inhibitory effects of aspirin, cilostazol and ramatroban on the release of P-selectin, TGF-β1 and TXA_2 from platelets in response to ADP (5 μmol/l), collagen and arachidonic acid are shown in Figure 4. When PRP was stimulated by ADP (5 μmol/l), 100 μmol/l aspirin significantly inhibited the release of TXA_2 compared with that of P-selectin and TGF-β1. In contrast, inhibitory effects of 10 μmol/l cilostazol and 1 μmol/l ramatroban on the release of TXA_2 in response to ADP (5 μmol/l) were similar to those on the release of P-selectin and TGF-β1. Aspirin and ramatroban markedly inhibited the release of P-selectin, TGF-β1 and TXA_2 to a similar degree in response to collagen and arachidonic acid. However, 10 μmol/l cilostazol inhibited the release of the three molecules in response to ADP, collagen and arachidonic acid to a similar degree.

Time-dependent change after blood collection and reproducibility in WB aggregation

In order to investigate the relationship between ADP concentration and pressure rate, WB aggregation induced by 1, 2, 4 and 8 μmol/l ADP was measured. As shown in Figure 5a, when control WB and aspirin-treated (10, 50, 100 and 500 μmol/l) WB were stimulated by ADP, the pressure rates in all samples increased depending on ADP concentrations. These data were presented as the dose–response plots for aspirin concentrations in Figure 5b. PATI values elevated with the increase in aspirin concentration. Figure 6 shows time-dependent changes in the PATI values after blood collection. PATI values immediately after blood collection (5 min) were 5.68 ± 1.71, and decreased gradually until 60 min after blood collection, and then increased slightly after 120 min. The following experiments to evaluate WB aggregation were performed using blood samples 60 min after collection. In the examination of reproducibility between two different sample days, the mean values of PATI from the same volunteers were 2.63 ± 0.65 and 2.52 ± 0.84 ($n = 8$), respectively, and no significant difference in PATI values between the two days was observed. While platelet counts from eight volunteers ranged from 17.5×10^4 to 31.2×10^4 cells/μl [mean platelet count, $(25.0 \pm 5.0) \times 10^4$ cells/μl], PATI values were in

Fig. 5

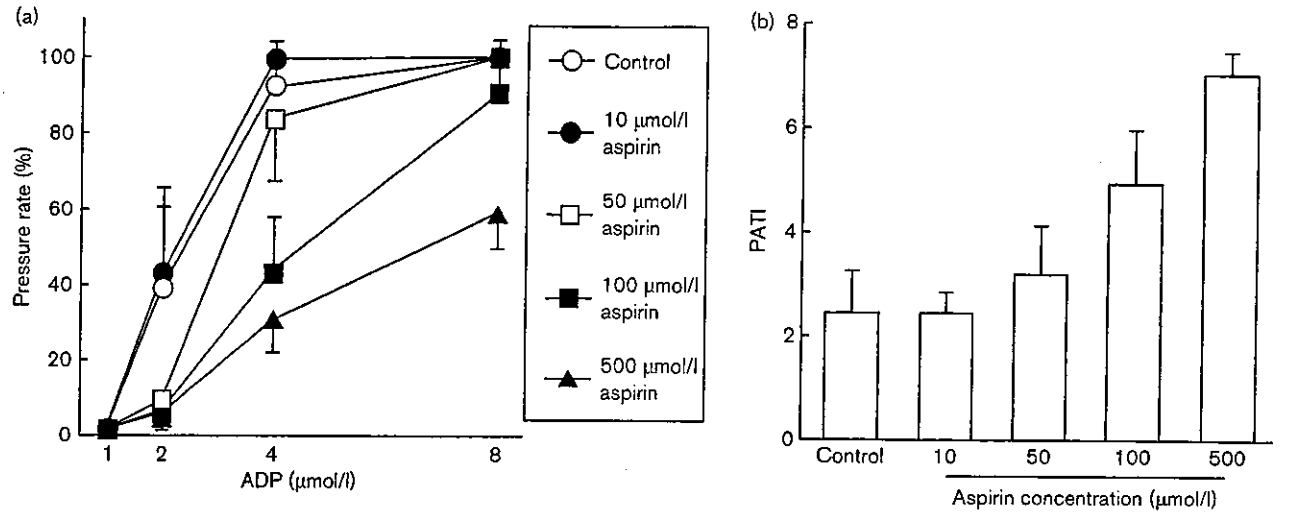

Relationship between adenosine diphosphate (ADP) concentration and pressure rate (%) in whole blood aggregation. Whole blood was pre-incubated with or without aspirin for 3 min prior to the addition of ADP (1, 2, 4 and 8 μmol/l). Whole blood aggregation was measured at 60 min after blood collection. Data represent mean ± standard deviation ($n = 8$). PATI, platelet aggregatory threshold index.

Fig. 6

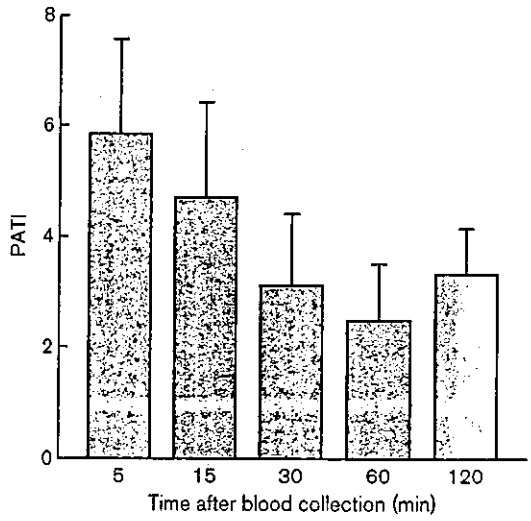

Time-dependent changes in platelet aggregatory threshold index (PATI) values after blood collection. Whole blood was stimulated by adenosine diphosphate (ADP) (1, 2, 4 and 8 μmol/l), and whole blood aggregation was measured at 5, 15, 30, 60 and 120 min after blood collection and PATI values were obtained. Data represent mean ± standard deviation ($n = 8$).

least three receptors: the P2X receptor that mediates rapid Ca ion influx, the P2Y1 receptor coupled to Gq-protein that stimulates phospholipase C (PLC) and induces shape change, and the P2TAC receptor coupled to the Gi-protein that inhibits adenylyl cyclase [32]. Since aspirin inhibited ADP-induced PRP aggregation to a certain degree in the present study, aspirin, a cyclooxygenase inhibitor, may cause the inhibition of PRP aggregation in response to ADP through the P2Y1 receptor. The effects of aspirin on platelet aggregation in response to collagen may be due to the inhibition of platelet activation via glycoprotein (GP) Ia/IIa (the $\alpha_2\beta_1$ integrin), CD36 (GPIV, also known as GPIIIb), or GPVI, which are collagen receptors and lead to PLCγ2 tyrosine phosphorylation and bring about TXA_2 formation [33]. GPIV may accelerate the rate of adhesion once platelets establish contact with collagen fibres via GPVI and GPIa/IIa [34]. Aspirin markedly inhibits PRP aggregation in response to arachidonic acid, because arachidonic acid is utilized in TXA_2 formation.

Next, we measured the levels of sP-selectin, TGF-β1 and TXB_2 in response to ADP, collagen and arachidonic acid. Aspirin markedly decreased TXB_2 levels compared with levels of sP-selectin and TGF-β1 in response to ADP. In contrast, the rates of decrease of TXB_2 by cilostazol and ramatroban were similar to those of sP-selectin and TGF-β1 in response to ADP. Furthermore, aspirin and ramatroban strongly inhibited the release of P-selectin, TGF-β1 and TXB_2 in response to collagen and arachidonic acid compared with the response induced by ADP. These results suggest that aspirin may inhibit not only TXA_2 formation via cyclooxygenase, but also could inhibit the release reaction of TXA_2 via activation of PLC. Stimulation of platelets by collagen and arachidonic acid induces TXA_2 production and the release reaction of intraplatelet substances. Ramatroban inhibits TXA_2 binding to the TXA_2 receptor on the surface of plate-

Table 2 Correlations between pressure rate in whole blood aggregometry and other independent variables from platelet-rich plasma (PRP) aggregometry

	Whole blood:PRP	Coefficients (*R*)	*P* value
Aspirin-treated samples	Pressure rate:MA	0.849	< 0.001
	Pressure rate:sP-selectin	0.897	< 0.001
	Pressure rate:TGF-β1	0.920	< 0.001
	Pressure rate:TXB_2	0.737	< 0.001
	PATI:PATI	0.920	< 0.001
Cilostazol-treated samples	Pressure rate:MA	0.761	< 0.001
	Pressure rate:sP-selectin	0.823	< 0.001
	Pressure rate:TGF-β1	0.766	< 0.001
	Pressure rate:TXB_2	0.785	< 0.001
	PATI:PATI	0.828	< 0.001
Ramatroban-treated samples	Pressure rate:MA	0.638	< 0.001
	Pressure rate:sP-selectin	0.768	< 0.001
	Pressure rate:TGF-β1	0.774	< 0.001
	Pressure rate:TXB_2	0.802	< 0.001
	PATI:PATI	0.894	< 0.001

MA, percentage maximum aggregation; sP-selectin, soluble P-selectin; TGF-β1, transforming growth factor-beta 1; TXB_2, thromboxane B_2; PATI, platelet aggregatory threshold index.

activation through a system linked to PLC [35]. Cilostazol inhibited the release of all the molecules in response to ADP, collagen and arachidonic acid in a similar fashion. These results may be due to the difference in pharmacological mechanisms between aspirin (a cyclooxygenase inhibitor), cilostazol (a phosphodiesterase III inhibitor) and ramatroban (a specific TXA_2 receptor antagonist). Different signal pathways in platelets most surely play important roles in these events.

Third, we examined the effects of these drugs on WB aggregation induced by ADP (1, 2, 4 and 8 μmol/l) using the newly developed WB aggregometer with the screen filtration pressure method, and the results were compared with those from PRP aggregation induced by the same agonist. To measure WB aggregation, some devices such as the PFA-100 [3,8], and the Ultegra Platelet Analyzer [3,9,10] have been developed. In the present study, a WB aggregometer with a microsieve made of nickel, 3.7 mm in diameter, with 300 openings/1 mm diameter area was used [15]. The pressure rate (%) of WB through the microsieve after stimulation by ADP (1, 2, 4 and 8 μmol/l) was measured. Although we did not compare data from this device with another WB aggregometer, it is reported that platelet aggregation data from the PFA-100 and the Ultegra correlated well to data from a four-channel Chrono-log Lumi-Aggregometer using PRP [10]. We obtained the result that the pressure rate (%) of WB through the microsieves and maximum aggregation rate (%) of PRP correlated closely. In addition, there were close correlations between PATI values from WB aggregation and PRP aggregation, and also between the pressure rate (%) of WB and the levels of molecules released from platelets. Therefore, we believe that data from the newly developed WB aggregometer bear a striking resemblance to other devices such as the PFA-100 and the Ultegra. Recently, the effects of anti-platelet drugs were successfully evaluated using the WB aggregometer with the screen filtration pressure method [16]. In the present study, we confirmed a high reproducibility of WB aggregation by this apparatus. On the other hand, the PATI value (which represents the concentration of ADP inducing a 50% pressure rate) was highest at 5 min after blood collection and then gradually decreased up to 60 min time, in accordance with previous reports [15,16]. Thus, the data from the WB aggregometer were variable over the time period studied. Although the reason why the PATI value varies depending on time has not yet been clarified, it is possible that a change in the responsiveness of receptors on blood cells or unstable anti-thrombotic physiological substances such as prostacyclin may be contributing factors [15]. Therefore, in clinical laboratories, it is necessary to decide on the time after blood collection determining WB aggregability in order to obtain accurate results. In addition, it is possible to use this device as a rapid bedside test by measuring immediately after blood collection.

In fact, clinical research on subjects who had taken aspirin for angina pectoris is now being conducted. Addition of ADP to WB samples collected from the patients was performed punctually 60 min after drawing blood. In our unpublished data, PATI values in WB aggregation on the seventh day after cessation of taking aspirin to prevent extra bleeding during surgery of coronary artery bypass grafting were lower than those in the aspirin-taking period (2.19 ± 1.33 versus 4.81 ± 2.03). These results suggest that the WB analyser with screen filtration pressure method is a useful instrument even in clinical aspects to evaluate the anti-platelet effects of drugs, as well as other devices.

Overexpression of mitochondrial manganese superoxide dismutase protects against radiation-induced cell death in the human hepatocellular carcinoma cell line HLE. *Cancer Res* 2001; **61**:5382–5388.

31 Majima HJ, Nakanishi-Ueda T, Ozawa T. 4-Hydroxy-2-nonenal (5-NHE) staining by Anti-HNE antibody. In: Armstrong D (editor): *Oxidants and antioxidants: ultrastructure and molecular biology protocols*. Totowa, New Jersey: Humana Press, 2002; pp. 31–34.

32 Geiger J, Honig-Liedl P, Schanzenbacher P, Walter U. Ligand specificity and ticlopidine effects distinguish three human platelet ADP receptors. *Eur J Pharmacol* 1998; **351**:235–246.

33 Asselin J, Gibbins JM, Achison M, Lee YH, Morton LF, Farndale RW, *et al.* A collagen-like peptide stimulates tyrosine phosphorylation of syk and phospholipase Cγ2 in platelets independent of the integrin $\alpha_2\beta_1$. *Blood* 1997; **89**:1235–1242.

34 Nakamura T, Jamieson GA, Okuma M, Kambayashi J, Tandon NN. Platelet adhesion to native type I collagen fibrils. Role of GPVI in divalent cation-dependent and -independent adhesion and thromboxane A_2 generation. *J Biol Chem* 1998; **273**:4338–4344.

35 Takahara K, Murray R, FitzGerald GA, FitzGerald DJ. The response to thromboxane A_2 analogues in human platelets. Discrimination of two binding sites linked to distinct effector systems. *J Biol Chem* 1990; **265**:6836–6844.

ARD Online First, published on November 26, 2004 as 10.1136/ard.2004.025445

Increased Expression of Humanin Peptide in Diffuse Type Pigmented Villonodular Synovitis. Implication of its Mitochondrial Abnormality

Kosei Ijiri, Hiromichi Tsuruga, Harutoshi Sakakima, Kazuo Tomita, Noboru Taniguchi, Kazuki Shimo-onoda, Setsuro komiya, Mary B. Goldring, Hideyuki J Majima, and Takami Matsuyama

Increased Expression of Humanin Peptide in Diffuse Type Pigmented Villonodular Synovitis Implication of its Mitochondrial Abnormality (Extended Report)

Kosei Ijiri,[1,2]MD, PhD, Hiromichi Tsuruga,[3]PhD, Harutoshi Sakakima,[1]PT, PhD, Kazuo Tomita,[5]PhD, Noboru Taniguchi,[4]MD, Kazuki Shimoonoda,[4]MD, Setsuro Komiya,[4]MD,PhD, Mary B. Goldring,[2]PhD, Hideyuki J. Majima ,[5]DDS, PhD, and Takami Matsuyama[3]MD, PhD

[1]Course of Physiotherapy, School of Health Science, Faculty of Medicine, Kagoshima University, Kagoshima, Japan

[2]Beth Israel Deaconess Medical Center, New England Baptist Bone & Joint Institute, Boston, MA

[3]Immunology and Medical Zoology, Graduate School of Medicine, Kagoshima University, Kagoshima, Japan

[4]Department of Neuro-Musculoskeletal Disorder, Kagoshima University Graduate School of Medicine and Dentistry, Kagoshima University.

[5]Department of Oncology, Kagoshima University Graduate School of Medicine and Dental Science, Kagoshima, Japan

Address correspondence and reprint requests to Kosei Ijiri,MD,PhD

Kagoshima university

8-35-1, Sakuragoka

Kagoshima

Japan

Tel:81-99-275-5381 Fax:81-99-265-4699

kijiri@bidmc.harvard.edu

Key Words; Pigmented Villonodular Synovitis, Mitochondria, Humanin

Objectives: To define the pathogenesis of pigmented villonodular synovitis (PVNS), we searched for highly expressed genes in primary synovial cells from PVNS patients.

Methods: Using a combination of subtraction cloning and Southern colony hybridization, highly expressed genes in PVNS were detected in the comparison with rheumatoid synovial cells. Northern hybridization was performed to confirm the differential expression of the humanin gene in PVNS.The expression of the humanin peptide was analyzed by Western blotting and immunohistochemistry. Electron microscopic immunohistochemistry was performed to investigate the distribution of this peptide within the cell.

Results: Sixty eight highly expressed genes were identified in PVNS. Humanin genes were strongly expressed in diffuse type PVNS, but were barely detected in nodular type PVNS, RA or OA. The presence of humanin peptide was identified in synovium from diffuse type PVNS and most of the positive cells were distributed in the deep layer of the synovial tissue. Double staining with anti-humanin and anti-heat shock protein 60 showed that humanin was expressed mainly in mitochondria. Electron microscopy revealed immunolocalization of this peptide predominantly around dense iron deposits within the siderosome.

Conclusions: Increased expression of the humanin peptide in mitochondria and siderosomes is the characteristic of synovial cells from diffuse type PVNS. Humanin is an anti-apoptotic peptide which is known to be encoded in the mitochondrial genome. Present findings suggest that mitochondrial dysfunction may be primary in the pathogenesis of diffuse type PVNS and that the humanin peptide may be involved in the neoplastic process in this form of PVNS.

Introduction

Pigmented Villonodular Synovitis (PVNS) is classified as an uncommon idiopathic proliferative synovial process. (1,2) It can exist in a localized form within a joint but more commonly occurs as a diffuse form where the entire synovium of a joint is affected. (3,4,5,6,7) The exact etiology of PVNS is still unknown.(8,9,10) Previous experimental and epidemiologic studies have suggested that PVNS is a reactive process involving a chronic inflammatory response. (11,12) However, recent studies showing the capacity of these lesions for autonomous growth and the potential for recurrence have suggested involvement of a neoplastic process. (13) The neoplastic hypothesis has been further supported by studies suggesting that heterogeneous proliferating cells, such as fibroblasts, histiocytes, multinuclear cells and chronic inflammatory cells, might be neoplastic, with other cell types being reactive in nature. (14,15)

Histologically, PVNS is composed of proliferating mononuclear cells, with frequent giant cells, and intracellular and extracellular iron deposits. These iron deposits are observed as membrane-bound particles in siderosomes. Interestingly, Schumacher et al.(16) and Ghadially et al.(18) reported that the siderosome fuses with mitochondria in deep synovial cells from PVNS patients. Moreover, abundant mitochondria throughout the cytoplasma were observed in dispersed stromal cells containing electron-dense inclusions and in giant cells.(16.18)

In the present study, we searched for highly expressed genes in primary synovial cells from PVNS patients compared to those from patients with RA. We supposed that the comparison of synovial cells from PVNS with those from RA, which are composed of chronic inflammatory

cells, would identify the distinct nature of PVNS and define this proliferative process more precisely. Ribosomal RNA (rRNA) with poly A tail encoded by mitochondrial genes were highly expressed in PVNS. Among these genes, humanin has been reported to act as an oncopeptide or as an anti-apoptotic factor against Bax (Bcl2-associated X protein), which is an apoptosis-inducing protein. (19,20) However, little is known about the pathological role of humanin in diseases other than Alzheimer's disease.

We report here that the expression of humanin peptide is increased strongly in diffuse type PVNS compared to other arthrides and it is abundant in mitochondria and siderosomes of synovial cells from PVNS.

Methods

Synovial tissue preparation and RNA extraction.

Synovial biopsy specimens were obtained during surgery from 6 patients with PVNS, 3 with RA and 3 with osteoarthritis (OA). These lesions were subtyped into two types (diffuse or nodular type) according to locations (intra-versus extraarticular) and pathological growth patterns, which reflected clinical characteristics and biological behavior. (13)

The RA patients met the criteria of the 1987 American College of Rheumatology. The tissue was cultured in IMDM with collagenase V(1mg/1ml medium) for 40 minutes and cells were harvested through mesh and gathered by centrifugation. Total cellular RNA was extracted using AGPC methods.(21) Equal aliquots were then electrophoresed on 1% agarose gels

stained with ethidium bromide to compare large and small rRNA qualitatively and to exclude degradation. Poly A^+ RNA was purified from total RNA using the First Track kit (Invitrogen).

Double-stranded cDNA synthesis and subtraction cloning. One μg of total RNA sample was used to synthesize full-length double-stranded cDNA using a SMART PCR cDNA Synthesis Kit (Clontech).Subtraction cloning was performed using a PCR-Select™ cDNA Subtraction Kit (Clontech). Equal amounts of double-stranded cDNAs from two patients with PVNS (diffuse type / lane 1, nodular type / lane2 in Fig.2) were used as tester cDNAs and equal amounts of double-stranded cDNAs from 3 RA patients were used as driver cDNAs.PCR using CD163 primers was performed to estimate the efficiency of subtraction and the expected decrease in CD163 abundance in the subtracted sample was observed (data not shown).

Southern colony hybridization.

Subtracted cDNAs were ligated to TOPO vector (Invitrogen) and transformed into DH10B cells (Invitrogen) by electroporation. After blue-white selection with X-gal containing LB plates, white colonies were cultured overnight with 150 μl LB medium in sterile 1.5 ml tubes and centrifuged for 2 min at 12000 g, and the pellet was resuspended in 10 μl LB medium. The medium was mixed completely and 2 μl were dotted on a nylon membrane for Southern hybridization. SMART double-stranded cDNA was labeled with [^{32}P]-dCTP by random priming (Stratagene). Membranes were hybridized in aqueous solution (5 x SCC, Denhardt's solution, 0.1% SDS, 10 mg salmon sperm DNA) overnight at 65°C. After washing at 65°C for 1 hour in 0.1 x SSC, 0.1% SDS, the membranes were exposed to X-ray film (Eastman

Kodak Co.) with an intensifying screen at -80°C. Quantitation of cDNA was performed by scanning with a BASS 1000 Densitometer (Fuji film), and normalization against GAPDH cDNA hybridized subsequently on the same blots.

DNA sequencing. Sixty eight cDNAs from differentially expressed clones were amplified with M13 reverse (5' CAGGAAACAGCTATGAC3') primers using thermal cycling conditions (96°C for 30 seconds, 50°C for 15 seconds, 60°C for 4 minutes for 25 cycles). The cDNAs were purified and sequenced using the ABI PRISM^{TM} Dye Terminator Cycle Sequencing Ready Reaction Kit with Template Suppression Reagent (ABI PRISM^{TM}). DNA sequences were analyzed using DNASIS software and compared to sequences in GeneBank (National Center for Biotechnology Information, Bethesda, MD).

Northern hybridization. Poly A^+ RNA (168 ng) samples of the synovium from 5 PVS, 3 RA and 3 OA patients were loaded and fractionated through 1.0 % agarose gels and transferred to Hybond^{TM}-N+ nylon transfer membrane (Amersham). Purified human cDNA (40 ng) was labeled with [^{32}P-dCTP] by random priming and applied to the membrane forhybridization in aqueous solution (5 x SCC, Denhardt's solution, 0.1% SDS, 10mg salmon sperm DNA, 50% formamide) overnightat 42°C. After washing at 42°C for 1 hour in 0.1 x SSC, 0.1% SDS, the membranes were exposed to X-ray film (Eastman Kodak Co.) with an intensifying screen at -80°C.

Semiquantitative Reverse Transcriptase Polymerase Chain Reaction (RT-PCR).

Total RNA (2.5 μg) from 5 patients with PVNS, 3 with RA and 2 with OA were used for cDNA

synthesis with oligo(dT)$_{12-18}$ as template primer using M-MuLV reverse transcriptase. The reaction was conducted in a final volume of 50 μl containing 1 ml of the transcribed cDNA probe, 200 μM of each dNTP, 1 X PCR buffer including 1.5 mM $MgCl_2$ (Takara Biomedical), 0.4 μM forward and reverse primers, and 2.5U Taq polymerase (Takara). All amplimers were amplified simultaneously with GAPDH as internal standard. The respective primer pairs were for cytochrome c (forward; 5'-GCATAAACAACATAAGCTTCTGA-3',reverse;5'-CAGCAGATCATTTCATATTGCTT-3'), for ATPase (forward; 5'-TCTCATCAACAACCGACTAATCA-3', reverse; 5'-GATAAGTGTAGAGGGAAGGTTAA-3'), for NADH dehydrogenase (forward; 5'-TTTACTCAATCCTCTGATCAGGG-3', reverse; 5'-CGAATTCATAAGAACAGGGAGGT-3'), and for cytochrome b (forward; 5'-AATTACAAACTTACTATCCGCCA-3', reverse; 5'-TGGGCGAAATATTATGCTTTGTT-3'). The reactions were incubated for 3 min at 94°C, followed by 32 cycles of denaturation for 1 min at 94°C, annealing for 1.5 min at 52°C, and extension for 1 min at 72°C.

Cell and tissue processing for light microscope and immunohistochemistry.

To isolate synovial cells, the deep layers of synovium from diffuse type of PVNS were cultured in IMDM with collagenase V(1mg/1ml medium) for 20 minutes and cells were harvested through mesh and gathered by centrifugation. These synovial cells were cultured in IMDM with 10% FBS for 4 hours and fixed with 10% buffered formaldehyde at room temperature for